Throughput Performance Enhancement for MUDiv/OFDMA using MMSE Equalization without Guard Interval

Yuta Ida[†], Chang-Jun Ahn, Takeshi Kamio, Hisato Fujisaka, and Kazuhisa Haeiwa

Abstract—**Recently, to achieve a high data rate and a high quality multimedia service, orthogonal frequency division multiplexing (OFDM) and orthogonal frequency division multiplexing access (OFDMA) are widely studied. In a wireless network, the transmitted signal of each user has independent channel fluctuation characteristics. By using such characteristic, a multiuser diversity (MUDiv) for OFDMA has been proposed. In a multipath fading environment, inter-symbol interference (ISI) is caused. In OFDM systems, the ISI is eliminated by inserting the guard interval (GI). On the other hand, this operation is degraded the maximum throughput. In this paper, we propose to enhance the throughput performance for a MUDiv/OFDMA without GI.**

Index Terms—**OFDMA, multiuser diversity, guard interval, MMSE, throughput**

I. Introduction

Orthogonal frequency division multiplexing (OFDM) systems have recently attracted considerable attention as a fourth generation mobile communication system due to the parallel signal transmission using many subcarriers that are mutually orthogonal [1]. Moreover, since the frequency spacing of each subcarrier minimum, OFDM can treat a frequency selective fading as a flat fading for each subcarrier [2], [3]. Furthermore, OFDM has been chosen for several broadband WLAN standard like IEEE802.11a, IEEE802.11g, and European HIPERLAN/2. In addition, terrestrial digital audio broadcasting (DAB) and digital video broadcasting (DVB) have also proposed for broadband wireless multiple access system such as IEEE802.16 wireless MAN standard and interactive DVB-T [4]-[6]. OFDM allows only one user on the channel at any given time. To accommodate multiple users, orthogonal frequency division multiple access (OFDMA) has been proposed [6]. OFDMA combines OFDM and frequency division multiple access (FDMA), and provides each user with a fraction of the available number of subcarriers. Worldwide interoperability for microwave access (WiMAX) as IEEE802.16 standard is applied an OFDMA to accommodate many users in the same channel at the same time [7], [8]. WiMAX is one of the next generation mobile networks designed to support a high capacity and a high data rate.

In a wireless network, the transmitted signal of each user has independent channel fluctuation characteristics. By using such characteristic, the diversity that exists between users is called multiuser diversity (MUDiv) and can be exploited by the sender to enhance the capacity of a wireless network [9]-[11]. Therefore, the MUDiv technique achieves dramatically increased the system throughput and the spectral efficiency [12]. In a MUDiv for OFDMA, the exploiting channel fluctuation diversity is in essence done by selecting the user with the strong subcarrier channels.

In a multipath fading environment, inter-symbol interference (ISI) and inter-carrier interference (ICI) are caused due to the previous symbol and different subcarrier, respectively. In OFDM systems, the ISI is eliminated by inserting the guard interval (GI) longer than the delay spread channel. However, this operation is degraded the maximum throughput due to the extended packet length. To mitigate this problem, the several methods without GI have been proposed [13]-[15]. For example, [13] improves the performance in the short GI. However, the system performance without GI is significantly degraded. [14] mitigates the complexity by using the time domain equalizer (TDE). However, TDE is degraded the system performance in the rugged environment as a frequency selective fading. [15] adapts the overlap-frequency domain equalization (FDE). However, the noise enhancement due to the residual ISI is not considered by using the perfect channel estimation. Previously, we have proposed the ISI and ICI compensation methods for multiple-input multiple-output (MIMO) systems [16]. To mitigate above-mentioned problems, in this paper, we propose a MUDiv/OFDMA without GI using the ISI and ICI cancellation to enhance the throughput performance. In Section II, we present a MUDiv/OFDMA system. The configuration of the proposed system is described in Section III. In Section IV, we show the computer simulation results. Finally, the conclusion is given in Section V.

II. MUDiv/OFDMA System

A. Channel Model

We assume that a propagation channel consists of L discrete paths with different time delays. The impulse response $h_m(\tau, t)$

Manuscript received May 10, 2011.

Y. Ida, T. Kamio, H. Fujisaka, and K. Haeiwa are with the Graduate School of Information Sciences, Hiroshima City University, 3-4-1 Ozukahigashi, Asaminami-ku, Hiroshima, 731-3194 Japan.

C. Ahn is with the Graduate School of Engineering, Chiba University, 1-33 Yayoi-cho, Inage-ku, Chiba, 263-8522 Japan.

e-mail: y.ida@chiba-u.jp[†]

for user m is represented as

$$h_m(\tau,t)=\sum_{l=0}^{L-1} h_{m,l}(t)\delta(\tau-\tau_{m,l}), \tag{1}$$

where $h_{m,l}$, $\tau_{m,l}$ are the complex channel gain and the time delay of the lth propagation path for user m, and $\sum_{l=0}^{L-1} E\left|h_{m,l}^2\right|=1$, where $E|\cdot|$ denotes the ensemble average operation. The channel transfer function $H_m(f, t)$ is the Fourier transform of $h_m(\tau, t)$ and is given by

$$\begin{aligned} H_m(f,t) &= \int_0^\infty h_m(\tau,t)\exp(-j2\pi f\tau)d\tau \\ &= \sum_{l=0}^{L-1} h_{m,l}(t)\exp(-j2\pi f\tau_{m,l}). \end{aligned} \tag{2}$$

B. *Subcarrier Selection*

Figure 1 shows the magnitude of the channel transfer function for different users in a single cell. Subcarriers fade differently from user to user in OFDMA systems. The diversity that exists between users is called multiuser diversity (MUDiv) and can be exploited by the transmitter to enhance the capacity of a wireless network. In a MUDiv/OFDMA, exploiting channel fluctuation diversity is in essence done by selecting the user with the strong subcarrier channels. In this case, the selection scheme is very important to select subcarriers with the highest SNR and to guarantee all users the same quality of service (QoS). The subcarrier selection criteria for each user is given by

$$Z=\sum_{m=0}^{N_u-1}\sum_{k=0}^{N_c-1}\left|H_m(k)\right|^2\alpha_{m,k},\ \alpha_{m,k}=\begin{cases}1 & \text{allocation}\\ 0 & \text{no allocation},\end{cases} \tag{3}$$

where $\alpha_{m,k}$ is the selection parameter, N_c is the number of subcarriers, and N_u is the number of users, respectively. From Eq. (3), the subcarrier is selected for the maximization of Z. In this case, one subcarrier is selected at once and users do not share the same subcarriers. Therefore, the MUDiv technique promises dramatically increased the system throughput and the spectral efficiency. On the other hand, Eq. (3) requires large complexity for calculating subcarrier assignment. To mitigate the complexity, the block selection method is considered. In the block selection, the block for each user is given by

$$H'_m(q)=\sum_{k=0}^{\beta-1}\frac{\left|H_m(\beta q+k)\right|^2}{N_b}, \tag{4}$$

where N_b is the block length, β is $\lfloor N_c/N_b \rfloor$, and $\lfloor y \rfloor$ denotes the largest integer less than or equal to y, respectively. By using Eq. (4), the block selection criteria for each user is given by

$$Z'=\sum_{m=0}^{N_u-1}\sum_{q=0}^{\beta-1}\left|H'_m(q)\right|^2\alpha_{m,q},\ \alpha_{m,q}=\begin{cases}1 & \text{allocation}\\ 0 & \text{no allocation}.\end{cases} \tag{5}$$

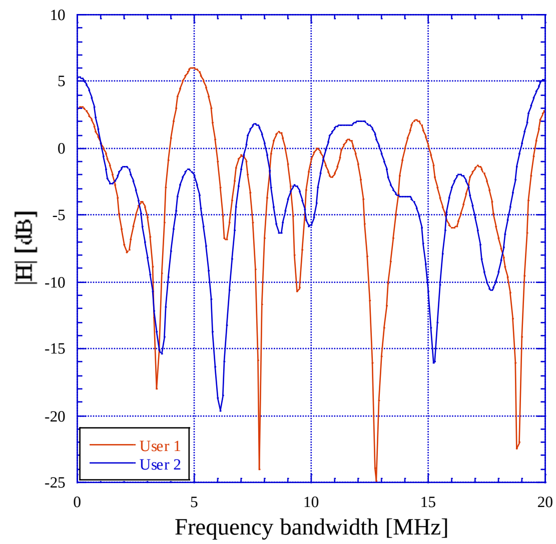

Fig. 1. Magnitude of the channel transfer function for a radio channel with multipath.

C. *MUDiv/OFDMA*

The transmitter block diagram of the proposed system is shown in Fig. 2(a). Firstly, the coded data is modulated and N_p pilot symbols are appended at the beginning of the sequence. The MUDiv/OFDMA transmitted signal for user m can be expressed in its equivalent baseband representation as

$$\begin{aligned} s_m(t)=\sum_{i=0}^{N_p+N_d-1} g(t-iT)\cdot\Bigg\{\sqrt{\frac{2S}{N_c}}\sum_{k=0}^{N_c-1}u_m(k,i) \\ \cdot\exp\left[j2\pi(t-iT)k/T_s\right]\Bigg\}, \end{aligned} \tag{6}$$

where N_d and N_p are the number of data and pilot symbols, T_s is the effective symbol length, S is the average transmission power, and T is the OFDM symbol length, respectively. The frequency separation between adjacent orthogonal subcarriers is $1/T_s$ and can be expressed, by using the kth subcarrier of the ith modulation symbol $d_m(k, i)$ with $|d_m(k, i)|=1$ for $N_p \le i \le N_p+N_d-1$, as

$$u_m(k,i)=c_{PN}(k)\cdot d_m(k,i), \tag{7}$$

where c_{PN} is a long pseudo-noise (PN) sequence as a scrambling code to reduce the peak average power ratio (PAPR). Moreover, the kth subcarrier $d_m(k, i)$ is given by

$$d_m(k,i)=\begin{cases}\sum_{q=0}^{N_b-1} x_m(\beta N_b+q,i) & \text{for } \beta\le\lfloor k/N_b\rfloor\le\beta+1\\ 0 & \text{otherwise},\end{cases} \tag{8}$$

where $x_m(k, i)$ is the kth subcarrier of the ith symbol for user m. In general, the GI is inserted in order to eliminate the ISI due to a multipath fading, and hence, we have

$$T=T_s+T_g, \tag{9}$$

where, T_g is the GI length. In Eq. (6), the transmission pulse $g(t)$ is given by

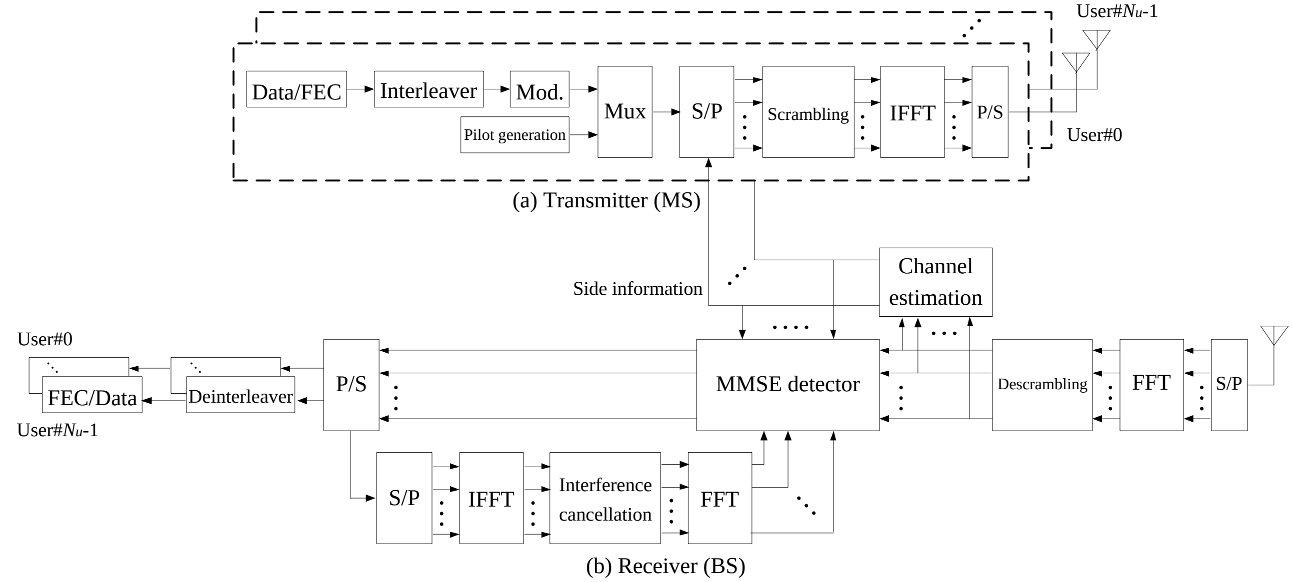

Fig. 2. Proposed system.

$$g(t)=\begin{cases}1 & \text{for } -T_g \le t \le T_s \\ 0 & \text{otherwise.}\end{cases} \tag{10}$$

The receiver structure is illustrated in Fig. 2(b). By applying the FFT operation, the received signal $r(t)$ is resolved into N_c subcarriers. The received signal $r(t)$ in the equivalent baseband representation can be expressed as

$$r(t)=\sum_{m=0}^{N_u-1}\int_{-\infty}^{\infty} h(\tau,t)s_m(t-\tau)d\tau+n(t), \tag{11}$$

where $n(t)$ is additive white Gaussian noise (AWGN) with a single sided power spectral density of N_0. The kth subcarrier $\tilde{r}(k,i)$ is given by

$$\begin{aligned}\tilde{r}(k,i)&=\frac{1}{T_s}\int_{iT}^{iT+T_s} r(t)\exp\left[-j2\pi(t-iT)k/T_s\right]dt \\ &=\sqrt{\frac{2S}{N_c}}\sum_{m=0}^{N_u-1}\sum_{e=0}^{N_c-1}u_m(e,i)\cdot\frac{1}{T_s}\int_0^{T_s}\exp\left[j2\pi\right. \\ &\quad\left.\cdot(e-k)t/T_s\right]\cdot\left\{\int_{-\infty}^{\infty}h(\tau,t+iT)g(t-\tau)\right. \\ &\quad\left.\cdot\exp(-j2\pi e\tau/T_s)d\tau\right\}dt+\hat{n}(k,i),\end{aligned} \tag{12}$$

where $\hat{n}(k,i)$ is AWGN noise with zero-mean and a variance of $2N_0/T_s$. After abbreviating, Eq. (12) can be rewritten as

$$\begin{aligned}\tilde{r}(k,i)&\approx\frac{1}{T_s}\sqrt{\frac{2S}{N_c}}\sum_{m=0}^{N_u-1}\sum_{e=0}^{N_c-1}u_m(e,i)\cdot\int_0^{T_s}\exp\left[j2\pi\right. \\ &\quad\left.\cdot(e-k)t/T_s\right]\cdot\left\{\int_{-\infty}^{\infty}h(\tau,t+iT)g(t-\tau)\right. \\ &\quad\left.\cdot\exp(-j2\pi e\tau/T_s)d\tau\right\}dt+\hat{n}(t) \\ &=\sqrt{\frac{2S}{N_c}}\sum_{m=0}^{N_u-1}H(k/T_s,iT)u_m(k,i)+\hat{n}(k,i).\end{aligned} \tag{13}$$

After descrambling, the output signal $r(k, i)$ is given by

$$\begin{aligned}r(k,i)&=\frac{c_{PN}^*(k)}{\left|c_{PN}(k)\right|^2}\tilde{r}(k,i) \\ &=\sqrt{\frac{2S}{N_c}}\sum_{m=0}^{N_u-1}H(k/T_s,iT)d_m(k,i)+\hat{n}(k,i),\end{aligned} \tag{14}$$

where $(\cdot)^*$ is a complex conjugate and $c_{PN}^*(k)/\left|c_{PN}(k)\right|^2$ is the descrambling operation, respectively. For Eq. (14), we can see that the received signal has the frequency distortion arising from a frequency selective fading. To mitigate this frequency distortion, the frequency equalization combining is necessary. For the channel estimation scheme using N_p pilot symbols, the channel response of the kth subcarrier is given by

$$\tilde{H}(k/T_s)=\frac{1}{N_p\sqrt{2P/N_c}}\sum_{i=0}^{N_p-1}r(k,i), \tag{15}$$

where P is the transmitted pilot signal power. Here, the combining weight for the kth subcarrier is denote by $\omega(k, i)$. After the frequency equalization combining, the received detected data symbol for user m can be written as

$$\begin{aligned}\tilde{d}_m(k,i)&=r(k,i)\cdot\omega(k,i) \\ &=\sqrt{\frac{2S}{N_c}}H(k/T_s,iT)d_m(k,i)\cdot\omega(k,i)+\hat{n}(k,i)\cdot\omega(k,i) \\ &\qquad \text{for } \beta\le\lfloor k/N_b\rfloor\le\beta+1.\end{aligned} \tag{16}$$

From Eq. (16), the decision variable of the kth subcarrier and the ith data symbol for user m is obtained by

$$\tilde{x}_m(k,i)=\sum_{q=0}^{N_b-1}\tilde{d}_m(\beta N_b+q,i) \quad \text{for } \beta\le\lfloor k/N_b\rfloor\le\beta+1. \tag{17}$$

III. Proposed System

A. MUDiv/OFDMA without GI

In the proposed system, we have Eq. (9) as

$$T = T_s . \tag{18}$$

In this case, the received signal $r(k, i)$ after the pilot signal separation contains the ISI and ICI. In this paper, we eliminate the ISI and ICI in the time domain. Firstly, the received signal $r(k, i)$ after the IFFT operation is rewritten the time domain matrix form as

$$\mathbf{R}_i = \sum_{m=0}^{N_u-1}\left(\boldsymbol{\lambda}_{isi,i-1}\mathrm{F}\mathbf{D}_{i-1,m} + \boldsymbol{\lambda}_{ici,i}\mathrm{F}\mathbf{D}_{i,m}\right) + \mathbf{N}_i , \tag{19}$$

where $\boldsymbol{\lambda}_{isi,i-1}$ and $\boldsymbol{\lambda}_{ici,i}$ are the $N_c \times N_c$ ISI and ICI channel matrices for the $(i - 1)$th and the ith symbols, F is the IFFT operation, and $\mathbf{N}_i$ is the $N_c \times 1$ noise matrix, respectively. In next subsection, we explain the ISI and ICI compensation methods.

B. ISI and ICI Equalization

In general, the first data symbol of the received signal has no the ISI [16]. Hence, the received signal of Eq. (19) for $i = 0$ is expressed as

$$\mathbf{R}_0 = \sum_{m=0}^{N_u-1}\boldsymbol{\lambda}_{ici,0}\mathrm{F}\mathbf{D}_{0,m} + \mathbf{N}_0 . \tag{20}$$

For $i > 0$, we eliminate the ISI and ICI. The ISI equalization is performed by using the previous detected signal $\tilde{\mathbf{D}}_{i,m}$. Therefore, the time domain signal $\tilde{\mathbf{R}}_i$ to eliminate the ISI is obtained by

$$\begin{aligned}\tilde{\mathbf{R}}_i &= \mathbf{R}_i - \sum_{m=0}^{N_u-1}\hat{\boldsymbol{\lambda}}_{isi,ici}\mathrm{F}\tilde{\mathbf{D}}_{i-1,m} \\ &= \sum_{m=0}^{N_u-1}\boldsymbol{\lambda}_{ici}\mathrm{F}\mathbf{D}_{i,m} + \tilde{\mathbf{N}}_i ,\end{aligned} \tag{21}$$

where $\hat{\boldsymbol{\lambda}}_{isi,ici}$ is the estimated ISI and ICI channel matrix and $\tilde{\mathbf{N}}_i$ is the noise term with the residual ISI, respectively. $\hat{\boldsymbol{\lambda}}_{isi,ici}$ is consisted the estimated channel impulse responses for Eq. (15) after the IFFT operation. After the FFT operation, the ISI equalized signal $\breve{\mathbf{D}}_{i,m}$ is generated by using Eq. (15). Observing Eq. (21), the ISI is eliminated. However, since the ICI is remained, the noise component is enhanced. Therefore, we mitigate the noise enhancement due to the ICI.

C. Replica Signal Insertion based on ICI Equalization

To avoid the noise enhancement due to the ICI, we consider the orthogonality reconstruction with inserting the eliminated signal due to the ISI compensation. The ICI equalized signal $\breve{\mathbf{R}}_i$ with inserting eliminated the part of the signal using previous detected signal $\breve{\mathbf{D}}_{i,m}$ is given by

$$\begin{aligned}\breve{\mathbf{R}}_i &= \tilde{\mathbf{R}}_i + \sum_{m=0}^{N_u-1}\hat{\boldsymbol{\lambda}}_{isi,ici}\mathrm{F}\breve{\mathbf{D}}_{i,m} \\ &= \sum_{m=0}^{N_u-1}\boldsymbol{\lambda}\mathrm{F}\mathbf{D}_{i,m} + \breve{\mathbf{N}}_i ,\end{aligned} \tag{22}$$

where $\boldsymbol{\lambda}$ is the time domain channel matrix and $\breve{\mathbf{N}}_i$ is the noise term with the residual ISI and residual ICI, respectively. After the FFT operation, the ICI equalized signal $\bar{\mathbf{D}}_{i,m}$ is generated by using Eq. (15). Observing Eqs. (21) and (22), the proposed method using the orthogonality reconstruction with inserting the subtracted signal due to the ISI compensation can mitigate the enhancement of the noise term. Therefore, the detected signal $\bar{\mathbf{D}}_{i,m}$ is accurately detected compared with $\breve{\mathbf{D}}_{i,m}$. Next, we explain that the frequency equalization combining using Eq. (15).

D. Zero Forcing (ZF)

The ZF weight $\omega_{zf}(k, i)$ is given by

$$\omega_{zf}(k,i) = \frac{1}{\tilde{H}(k/T)}. \tag{23}$$

Here, the time domain matrix $\breve{\mathbf{R}}_i$ after the FFT operation is rewritten the kth subcarrier $\breve{r}(k,i)$. By using Eq (23), the detectd signal $\bar{d}_{zf,m}(k,i)$ can be written as

$$\begin{aligned}\bar{d}_{zf,m}(k,i) &= \breve{r}(k,i)\cdot\omega_{zf}(k,i) \\ &= \sqrt{\frac{2S}{N_c}}\sum_{m=0}^{N_u-1}H(k/T, iT)d_m(k,i)\cdot\omega_{zf}(k,i) \\ &\quad + \bar{n}(k,i)\cdot\omega_{zf}(k,i) \\ &= \sqrt{\frac{2S}{N_c}}\sum_{m=0}^{N_u-1}\eta_{zf}(k,i)d_m(k,i) + \frac{\bar{n}(k,i)}{\tilde{H}(k/T)} \\ &\qquad \text{for } \beta \le \lfloor k/N_b \rfloor \le \beta + 1,\end{aligned} \tag{24}$$

where $\eta_{zf}(k,i) = H(k/T, i)/\tilde{H}(k/T)$ and $\bar{n}(k,i)$ is the noise term, respectively. From Eq. (24), the decision variable is obtained by

$$\bar{x}_{zf,m}(k,i) = \sum_{q=0}^{N_b-1}\bar{d}_{zf,m}(\beta N_b + q, i) \quad \text{for } \beta \le \lfloor k/N_b \rfloor \le \beta + 1. \tag{25}$$

The ZF scheme can restore the orthogonality, but it enhances the noise term due to the residual ISI and ICI.

E. Minimum Mean Square Error (MMSE)

The MMSE weight is given by

$$\omega_{mm}(k,i) = \frac{\tilde{H}^*(k/T)}{\left|\tilde{H}(k/T)\right|^2 + \tilde{\sigma}^2}, \tag{26}$$

where $\tilde{\sigma}^2$ is the estimated noise power. In this paper, by using the detected signal $\bar{d}_{zf,m}(k,i)$, $\tilde{\sigma}^2$ is obtained by

$$\tilde{\sigma}^2 = \frac{1}{N_d}\sum_{m=0}^{N_u-1}\sum_{i=0}^{N_d-1}\left|\acute{r}(k,i) - \tilde{H}(k/T)\bar{d}_{zf,m}(k,i)\right|^2. \quad (27)$$

By using Eq. (26), the detected signal $\bar{d}_{mm,m}(k,i)$ can be written as

$$\begin{aligned}\bar{d}_{mm,m}(k,i) &= \acute{r}(k,i)\cdot\omega_{mm}(k,i)\\ &= \sqrt{\frac{2S}{N_c}}\sum_{m=0}^{N_u-1}H(k/T,iT)d_m(k,i)\cdot\omega_{mm}(k,i)\\ &\quad +\bar{n}(k,i)\cdot\omega_{mm}(k,i)\\ &= \sqrt{\frac{2S}{N_c}}\sum_{m=0}^{N_u-1}\eta_{mm}(k,i)d_m(k,i)+\frac{\bar{n}(k,i)\cdot\tilde{H}^*(k/T)}{\left|\tilde{H}(k/T)\right|^2+\tilde{\sigma}^2}\\ &\qquad \text{for } \beta\le\lfloor k/N_b\rfloor\le\beta+1, \quad (28)\end{aligned}$$

where $\eta_{mm}(k,i) = \left\{H(k/T,T)\cdot\tilde{H}^*(k/T)\right\}/\left\{\left|\tilde{H}(k/T)\right|^2+\tilde{\sigma}^2\right\}$. Observing the noise term of Eqs. (24) and (28), the MMSE scheme can mitigate the noise enhancement due to the residual ISI and ICI. Therefore, the MMSE scheme is accurately detected to compare with the ZF scheme. Finally, the decision variable is obtained by

$$\bar{x}_{mm,m}(k,i) = \sum_{q=0}^{N_b-1}\bar{d}_{mm,m}(\beta N_b+q,i) \quad \text{for } \beta\le\lfloor k/N_b\rfloor\le\beta+1. \quad (29)$$

IV. Computer Simulated Results

In this section, we show the performance of the proposed method. Figure 2 shows a simulation model of the proposed system. On the transmitter, the data stream is encoded. Here, convolutional codes (rate R = 1/2, constrain length K = 7) with interleaving used. These have been found to be efficient for transmission of an OFDM signal over a frequency selective fading channel. The coded bits are QPSK modulated, and then the pilot signal and the data signal are multiplexed. After serial to parallel (S/P) converted, the OFDM signal is allocated based on Eq. (5). The scrambling operation is adapted to reduce the PAPR with a PN code. The OFDM time signal is generated by an IFFT. The transmitted signal is subject to broadband channel propagation. In this simulation, we assume that OFDM symbol period is 8.96 μs, and L = 5 path Rayleigh fadings have exponential shapes and a path separation T_{path} = 140 ns. The

TABLE I

Simulation Parameters.

Data modulation	QPSK
Data detection	Coherent
Symbol duration	8.96 μs
Frame size	N_p = 2, N_d = 20
FFT size	64
Number of carriers	64
Number of users	4
Guard interval	16 sample times
Fading	5 path Rayleigh fading
Doppler frequency	10 Hz
FEC	Convolutional code (R = 1/2, K = 7)

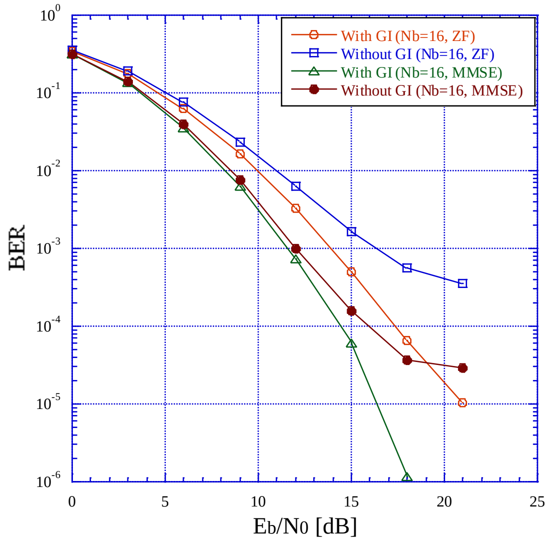

Fig. 3. The BER of the conventional MUDiv/OFDMA with the GI and without the GI at Doppler frequency of 10 Hz.

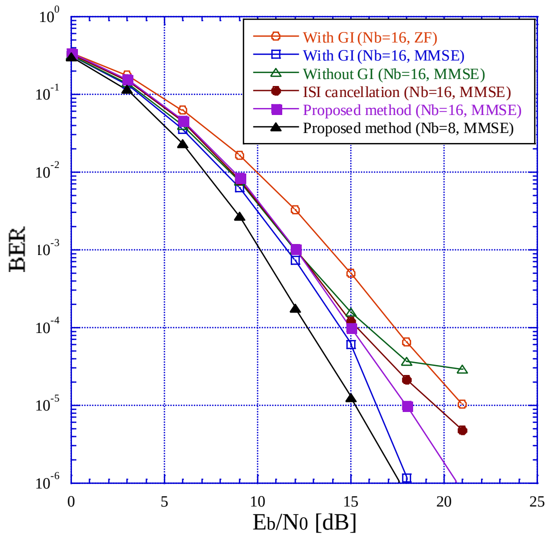

Fig. 4. The BER of the conventional methods and the proposed method for N_b = 8, 16 at Doppler frequency of 10 Hz.

maximum Doppler frequency is 10 Hz. In the receiver, the received signal is S/P converted. The parallel sequences are passed to the FFT operator and convert the signal back to the frequency domain. The frequency domain data signal is detected and demodulated. Since the detected signal contains the ISI and ICI, it is necessary to eliminate them. The ISI equalization is performed with the previous detected signal as Eq. (21). Moreover, to restrict the orthogonality, the ICI equalization is performed to insert the replica signal as Eq. (22). Finally, the MMSE equalization is performed to mitigate the noise enhancement due to the residual ISI and ICI as Eq. (28). After the detection, bits are decoded by using the Vitebi soft decoding algorithm. The packet consists of N_p = 2 and N_d = 20 data symbols. Table I shows the simulation parameters.

Fig. 3 shows the BER of the conventional MUDiv/OFDMA with and without GI at Doppler frequency of 10 Hz. For inserting GI, MMSE shows about 5 dB gain compared with ZF.

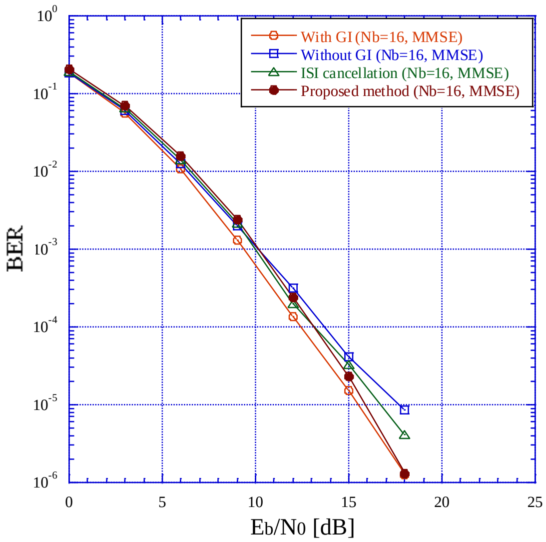

Fig. 5. The BER of the conventional methods and the proposed method for N_b = 16 in the perfect channel at Doppler frequency of 10 Hz.

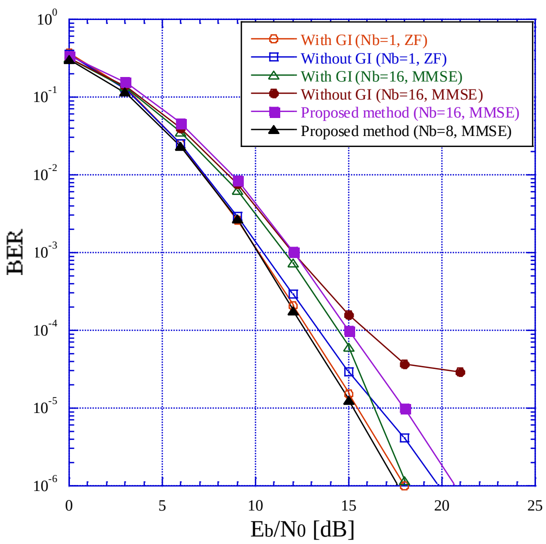

Fig. 6. The BER of the conventional methods and the proposed method for N_b = 1, 8, 16 at Doppler frequency of 10 Hz.

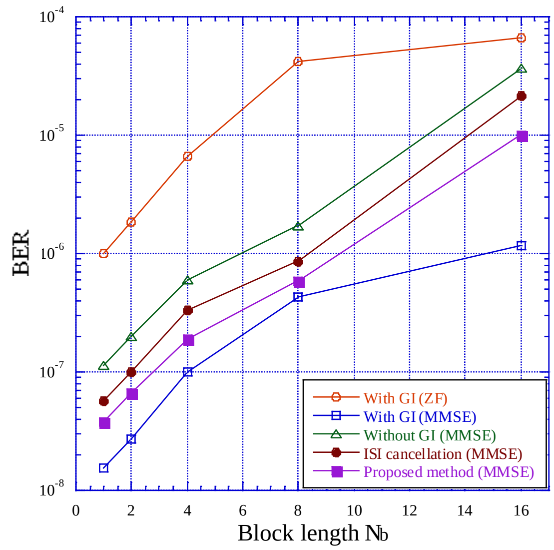

Fig. 7. The BER versus the block length N_b for the conventional methods and the proposed method with E_b/N_0 = 18 dB at Doppler frequency of 10 Hz.

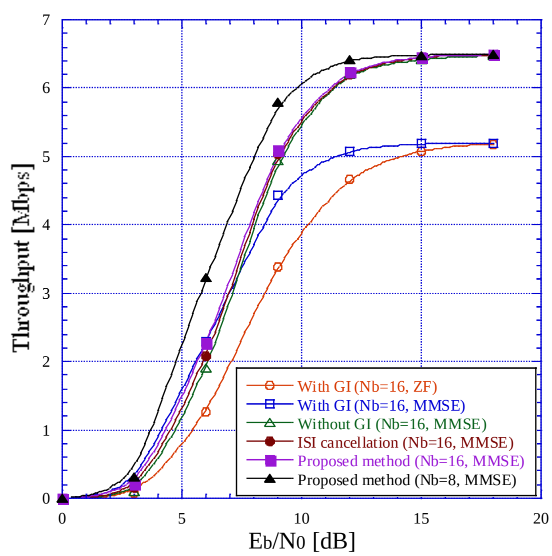

Fig. 8. The throughput of the conventional methods and the proposed method for N_b = 8, 16 at Doppler frequency of 10 Hz.

Moreover, MMSE shows about 8 dB gain compared with ZF without inserting GI. Therefore, the MMSE equalization can enhance the BER performance both inserting GI and without GI.

Figs. 4, 5, and 6 show the BER of the conventional methods and the proposed method at Doppler frequency of 10 Hz. In Fig. 4, the BER performance of ISI cancellation without GI shows about 6 times improvement compared with not inserting GI since ISI is eliminated. Moreover, the ISI cancellation shows about 2 times improvement compared with inserting GI with ZF. The BER performance of the proposed method for N_b = 16 shows about 6 times improvement compared with ISI cancellation without GI. However, the proposed method of N_b = 16 shows about 3 dB penalty compared with inserting GI with MMSE since the noise is enhanced due to the residual ISI and ICI. On the other hand, the proposed method of N_b = 8 shows the best BER performance. It means that a strong multiuser diversity can enhance the BER performance. In Fig. 5, the BER performance is improved under the perfect channel estimation. This is because the channel response of Eq. (15) is not contained the noise and the noise enhancement is mitigated. Therefore, the proposed method shows the approximately same BER performance compared with inserting the case with GI in the same block length. In Fig. 6, the BER of N_b = 1 shows a good performance, but large complexity is required. The BER performance of N_b = 1 with ZF shows about 67 times compared with MMSE of N_b = 16 for not inserting GI. On the other hand, the proposed method of N_b = 8 shows the approximately same BER performance compared with ZF for N_b = 1 with inserting GI. Therefore, the proposed method of N_b = 8 achieves the same BER performance compared with ZF for N_b = 1with inserting GI.

Fig. 7 shows the BER versus the block length N_b for the conventional methods and the proposed method with E_b/N_0 = 18 dB at Doppler frequency of 10 Hz. For N_b = 16, the proposed method shows about 7 times improvement compared with ZF with inserting GI. However, this shows about 9 times penalty compared with inserting GI of MMSE. For $N_b \leq 8$, the BER of proposed method approaches the BER performance of MMSE with inserting GI. Therefore, a multiuser diversity is effective to mitigate the ISI and ICI for $N_b \leq 8$.

Fig. 8 shows the throughput of the conventional methods and the proposed method at Doppler frequency of 10 Hz. The throughput T_{tp} is defined as

$$T_{tp} = \frac{N_d \cdot N_c \cdot C \cdot R}{\left(N_p + N_d\right) \cdot T} \cdot \left(1 - P_{per}\right), \tag{30}$$

where C is the modulation level and P_{per} is the packet error rate , respectively. In this simulation, we assume that the GI length is $T_s/4$. In this case, the symbol duration T is 11.2 μs, and the maximum throughput with GI would be 20 % degraded from Eq. (30). Thus, the maximum throughput of the proposed method for N_b = 16 shows the improvement of about 20 % compared with inserting GI. Therefore, the proposed method of N_b = 16 achieves the enhancement of the maximum throughput. Moreover, the proposed method of N_b = 8 shows the best throughput performance. This means that a strong multiuser diversity also enhances the throughput performance.

V. Conclusion

In this paper, we have proposed the ISI and ICI compensations to enhance the throughput performance for a MUDiv/OFDMA without GI. When the GI is not inserted, the system performance is significantly degraded due to the ISI and ICI. Therefore, we have performed ISI and ICI compensations. From the simulation results, the proposed method shows the approximately same BER performance compared with the case with inserting GI. For the throughput performance, the proposed method improves about 20 % compared with the case with inserting GI. As a result, the proposed method achieves the enhancement of the maximal throughput. Moreover, the proposed method of N_b = 8 shows the best performance both the BER and the throughput. Therefore, a strong multiuser diversity enhances the BER and the throughput performances.

References

[1] 2010 White paper information and communications in Japan, http://www.soumu.go.jp/johotsusintokei/whitepaper/ja/h22/pdf/index.html

[2] L. Cimini, “Analysis and simulation of digital mobile channel using OFDM”, IEEE Trans. Commun., vol. 33, no. 7, pp. 666-675, July 1985.

[3] J.A.C. Bingham, “Multicarrier modulation for data transmission: an idea whose time has come”, IEEE Commun. Mag., vol. 28, pp. 5-14, May 1990.

[4] ETSI ETS 301 958, “Digital video broadcasting (DVB); interaction channel for digital terrestrial television (RCT) incorporating multiple access OFDM”, ETSI, Tech. Rep., March 2002.

[5] “IEEE draft standard for local and metropolitan area network-part 16: Air interface for fixed broadband wireless access systems - medium access control modifications and additonal physical layer specifications for 2-11GHz”, IEEE LAN MAN Standards Committee, 2002.

[6] I. Koffman and V. Roman, “Broadband wireless access solutions based on OFDM access in IEEE802.16”, IEEE Commun. Mag., vol. 40, pp. 96-103, April 2002.

[7] WiMax Forum, http://www.wimaxforum.org/

[8] S. J. Vaughan-Nichols, “Mobile WiMax: the next wireless battleground?”, IEEE Computer Society, vol. 41, no. 6, pp. 16-18, June 2008.

[9] W. Seo, H. Song, J. Lee, and D. Hong, “A new asymptotic analysis of throughput enhancement from selection diversity using a high SNR approach in multiuser systems”, IEEE Trans. on Wireless Commun., pp. 55-59, vol. 8, no. 1, Jan. 2009.

[10] S. Kwack, H. Seo, and B. G. Lee, “Suitability-based subcarrier allocation for multicast services employing layered video coding in wireless OFDM System”, Proc. of VTC2007, pp. 1752-1756, Oct. 2007.

[11] J. Hui and Y. Zhou, “Enahanced rate adaptive resource allocation scheme in downlink OFDMA system”, Proc. of VTC2006, vol. 5, pp. 2464-2468, May 2006.

[12] C. Ahn, “Reinforced multiuser diversity using frequency symbol spreading and adaptive subcarrier block selection for OFDMA”, IEICE Technical Report, vol. 109, no. 266, CS2009-44, pp. 13-18, Nov. 2009.

[13] S. Trautmann and N. J. Fliege, “Perfect equalization for DMT systems without guard interval”, IEEE Journal on Selected Areas in Commun., pp. 987-996, nol 20, no. 5, June 2002.

[14] G. Mkrtchyan, K. Naito, K. Mori, and H. Kobayashi, “ML time domain channel estimation and equalization for OFDM without guard interval”, Proc. of ECTI-CON2005, pp. 473-476, May 2005.

[15] T. Kobori and F. Takehata, “An application of frequency diversity to OFDM transmission based on overlap-FDE”, IEICE Trans. Commun., vol. J93-B, no. 12, pp. 1651-1659, Dec. 2010.

[16] Y. Ida, C. Ahn, K. Kamio, H. Fujisaka, and K. Haeiwa, “Large delay spread cancellation based on replica signal for HTRCI-MIMO/OFDM”, Proc. of WPMC’09, S-11-4, pp. 1-5, Sep. 2009.